Optics Letters

High spectral density transmission emulation using amplified spontaneous emission noise

Daniel J. Elson,* Lidia Galdino, Robert Maher, Robert I. Killey, Benn C. Thomsen, and Polina Bayvel

Optical Networks Group, Department of Electronic & Electrical Engineering, University College London, Torrington Place, London WC1E 7JE, UK
**Corresponding author: uceedel@ucl.ac.uk*

Received 15 October 2015; revised 11 November 2015; accepted 20 November 2015; posted 20 November 2015 (Doc. ID 251121); published 18 December 2015

We demonstrate the use of spectrally shaped amplified spontaneous emission (SS-ASE) noise for wideband channel loading in the investigation of nonlinear transmission limits in wavelength-division multiplexing transmission experiments using Nyquist-spaced channels. The validity of this approach is explored through statistical analysis and experimental transmission of Nyquist-spaced 10 GBaud polarization-division multiplexing (PDM) quadrature phase-shift keying and PDM-16-ary quadrature amplitude modulation (QAM) channels, co-propagated with SS-ASE over single mode fiber. It is shown that this technique, which is simpler to implement than a fully modulated comb of channels, is valid for distances exceeding 240 km for PDM-16QAM with dispersion of 16 ps/nm/km, yields a good agreement with theory, and provides a conservative measure of system performance.

OCIS codes: (060.2330) Fiber optics communications; (060.2380) Fiber optics sources and detectors; (060.2430) Fibers, single-mode; (060.4080) Modulation; (060.1660) Coherent communications.

http://dx.doi.org/10.1364/OL.41.000068

The demand for internet bandwidth is ever increasing and research is focusing on exploring the limits of achievable capacity in optical fiber systems. The capacity is ultimately limited by the available bandwidth, constrained by the optical amplifiers, and the signal-to-noise ratio (SNR). In fiber systems, the optical nonlinearity also impacts on the throughput as it introduces additional distortion that depends on the power spectral density (PSD) of the transmitted signals. To maximize the throughput, irrespective of the amplifier technology, research on future optical systems seeks to maximize the information spectral density by using a combination of Nyquist pulse shaping [1] and employing higher cardinality modulation formats [2]. To assess the performance of these systems and robustness to nonlinear optical impairments, stemming from interchannel effects, it is necessary to fill the entire available transmission bandwidth with data channels.

The conventional experimental approach is to generate a single test channel, or several closely spaced channels, known as superchannels, over a spectral range less than the available transmission bandwidth [3]. The remaining transmission bandwidth or unused frequencies are then loaded with sources that are typically not identical to the spectrally efficient channel under test. Fully loading, such systems can require a large bank of laser sources, modulators, and schemes to overcome data correlation issues [4]. An alternative is to use spectrally shaped amplified spontaneous emission (SS-ASE) noise from an erbium-doped fiber amplification (EDFA) (or ASE from any other amplifiers), in place of the modulated laser bank for channel loading the transmission system. This scheme has the benefit over typical systems of having a lower complexity and requiring significantly less hardware and physical space and saving time in setup and monitoring. In addition, the incoherent nature of the ASE source removes the need for the decorrelation schemes that are typically involved in systems that use bulk modulation to emulate independent channels.

SS-ASE has previously been applied to power loading of optical amplifier chains [5], but without investigation or qualification of its validity limits, and as interfering channels in a conventional widely spaced (100 GHz) wavelength-division multiplexing (WDM) transmission system [6]. When compared to conventional modulated-data channel loading, ASE-based channel loading was shown to give a pessimistic performance estimate for quadrature phase-shift keying (QPSK) modulation and good agreement for orthogonal frequency division multiplexing (OFDM) [6]. Numerical simulations and analytical modeling of modulation format-dependent nonlinear interference noise was performed in [7] and have shown that, in dispersion uncompensated links, the nonlinear noise power is a function of modulation format. When OFDM or higher-order modulation formats (whose amplitude distributions tend toward a Gaussian distribution) are used, a larger nonlinear noise contribution can result. Hence, as the amplitude distribution of SS-ASE is Gaussian, its impact on the channel under test is expected to be similar to that of OFDM or higher-order modulation format data channels.

In this work, we investigate the use of SS-ASE to emulate interfering channels in a high spectral density Nyquist-spaced transmission system. First, a statistical analysis of the electrical-field-amplitude distribution in uncompensated links was carried out to compare the evolution of probability density

functions (PDFs) for modulated data signals with SS-ASE. Second, we experimentally explored the use of SS-ASE with a uniform PSD and show that it can be used to effectively emulate interferers in a Nyquist-spaced polarization-division multiplexing 16-ary quadrature amplitude modulation (PDM-16QAM) optical transmission system. Finally, we experimentally show that modulation format-dependent noise occurs at the beginning of a transmission link, within the first 240 km for Nyquist PDM-16QAM and 320 km for Nyquist PDM-QPSK over single mode fiber (SMF).

In dispersion-uncompensated links, one source of discrepancy between the Gaussian noise model and system performance comes from the modulation format-dependence of the nonlinear distortion [7]. For ASE to work as a valid interferer, the channel under test must have accumulated sufficient dispersion and/or be a higher-order modulation format. To investigate the suitability of SS-ASE for use as a substitute channel, a statistical analysis has been conducted, and the evolution of the electric-field PDFs has been evaluated. This allows quantification of how much accumulated dispersion is required for each format's PDF to evolve into a steady state. It has been shown that without dispersion, the In-Phase (I) and (Q) Quadrature components of PDM-QPSK evolve into a Gaussian distribution after transmission over 500 km of SMF [8].

To investigate this, two independent sets of data channels, modulated with Nyquist pulse shaped QPSK and 16QAM channels, and an SS-ASE channel were generated and compared. A pseudo-random binary sequence (PRBS) was used to generate PDM-QPSK and 16QAM channels, at 10 GBaud and two samples per symbol, and then Nyquist pulse shaped with a root raised cosine (RRC) filter with roll-off factor of 0.001 as shown in [1] to obtain minimum subchannel spacing without crosstalk and a spectrally flat superchannel that matches SS-ASE. The electric field was oversampled to eight samples per symbol to avoid simulation artifacts. The launch power was set to −10 dBm per channel [launch power was swept from −20 to 0 dBm in simulation with no significant change in statistical evolution; the electric field is dominated by dispersion rather than the nonlinear distortion at these powers]. To realize an SS-ASE channel, white Gaussian noise was generated as I and Q elements of the electric field. This gives rise to a Rayleigh distribution in the absolute value of the electric field, as shown in Fig. 1.

This is followed by a 10 GHz "brick-wall" bandpass filter to achieve a signal with the same spectral width as the modulated data channels. The power was set to match the PSD of the PDM-QPSK and 16QAM channels. The PDFs, shown in Figs. 1(a) and 1(b), were taken of the power-normalized electric field, which is the absolute value of the electric field divided by the square root of the averge power in the channel, such that the PDF does not scale as the signal power varies with fiber loss. The signal distributions at the transmitter are shown in Fig. 1(a). The PDM-QPSK and PDM-16QAM signals are to be expected to show one and three peaks, respectively, in electric-field magnitude as the symbols have discrete amplitudes. However, as can be seen from Fig. 1(a), the peaks are noticeably broadened due to the Nyquist pulse shaping.

Propagation over fiber was evaluated using the split-step Fourier method to solve the nonlinear Schrödinger equation with a step size of 0.1 km. The fiber parameters were set as follows: dispersion 16 ps/(nm.km), attenuation 0.16 dB/km, and nonlinear coefficient 1.1 $(\mathrm{Wkm})^{-1}$. The fiber span length

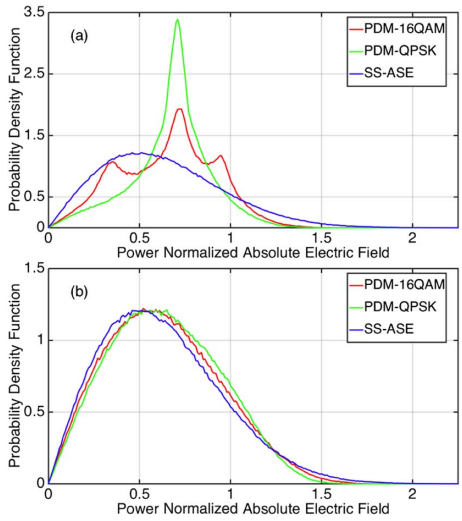

Fig. 1. Probability density functions of the absolute electric field for SS-ASE, Nyquist pulse shaped PDM-16QAM and PDM-QPSK at (a) transmitter and (b) after 240 km of fiber propagation.

was 80 km, and an EDFA with 5 dB noise figure was implemented to compensate for the fiber loss.

The field amplitude distribution of the three signals after propagation over 240 km is shown in Fig. 1(b). It can be seen that, due to accumulated dispersion, noise and fiber nonlinearity, the PDM-QPSK and PDM-16QAM signal-amplitude distributions have almost converged to that of the SS-ASE. After this distance, the SS-ASE, PDM-16QAM, and PDM-QPSK signals have variances with similar values of 0.108, 0.099, and 0.095, respectively. To characterize this, the evolution of peak to average ratio (PAR) of absolute value of electric field with propagation distance is shown in Fig. 2. It can be seen that the SS-ASE's PAR does not change upon transmission, but both the PDM-16QAM and PDM-QPSK signals converge to the same ratio as the SS-ASE. The PDM-QPSK has a higher initial PAR and converges to SS-ASE after approximately 240 km, while the PDM-16QAM takes only 180 km. This means any deviation from the Gaussian noise model should occur in the first 240 km while the electric field distributions are dissimilar. Accumulated dispersion is a function of bandwidth, so PAR convergence distance is shorter for higher symbol rate channels. If partial dispersion compensation is used above this distance, the PAR curves can diverge, leading to further penalty.

The experimental setup used to investigate this behavior is shown in Fig. 3(a). A superchannel was used as the channel under test and its generation was identical to that described

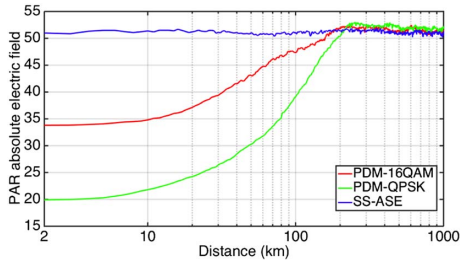

Fig. 2. Peak to average ratio (PAR) of the absolute electric field as a function of distance for PDM-QPSK, PDM-16QAM, and SS-ASE.

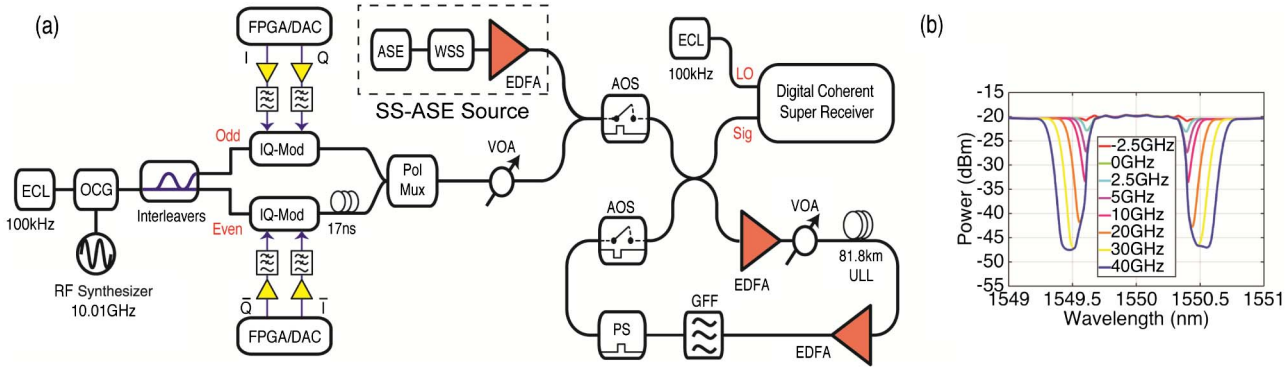

Fig. 3. (a) Overall system setup consisting of an external cavity laser (ECL), optical comb generator (OCG), IQ modulators, and polarization multiplexer (Pol Mux). The recirculation loop uses acousto-optic switches (AOS), a gain flattening filter (GFF), variable optical attenuators (VOA), an ultralow loss (ULL) fiber, and a polarization scrambler (PS). (b) Optical spectra of SS-ASE and nine subchannel superchannel with various guardbands.

in [1]. The SS-ASE was generated from an ASE noise source and was launched into a wavelength selective switch (WSS), followed by an EDFA with an output power of 19 dBm. The WSS was used to limit the bandwidth of the ASE noise source and flatten the ASE spectral profile by pre-emphasizing for the gain profile of the following EDFA. The SS-ASE was then combined with the superchannel source using a 3 dB coupler. The PSD of the SS-ASE noise and the superchannel were matched to within 0.3 dB, as shown in Fig. 3(b). The power of the combined signal was measured using an optical spectrum analyzer with a resolution of 0.1 nm. This enables emulation of a reconfigurable number of SS-ASE channels with arbitrary spacing and bandwidth.

For transmission, a recirculating optical fiber loop was used to evaluate SS-ASE as interfering data channels. It consisted of a single 81.7 km span of Corning SMF-28 ULL fiber, with a loss of 0.165 dB/km, dispersion ≤18 ps/nm/km, a gain flattening filter (GFF), a polarization scrambler, and two EDFAs with a noise figure of 5 dB. The EDFA before the fiber span had a maximum output power of 24 dBm, enabling a maximum launch power of −2 dBm per channel when filling 810 GHz of bandwidth. The optical signal was received using a polarization diverse coherent receiver and 100 kHz linewidth external cavity laser (ECL) as a local oscillator. The channels were captured using a 160 GS/s real-time sampling oscilloscope with 63 GHz of analog electrical bandwidth. Subsequently the channels were processed digitally as in [1] for linear impairment. Error counting was performed and the Q^2-factor was calculated from the measured bit error rate (BER).

The back-to-back (BTB) performance was measured to verify the impact of combining the superchannel with

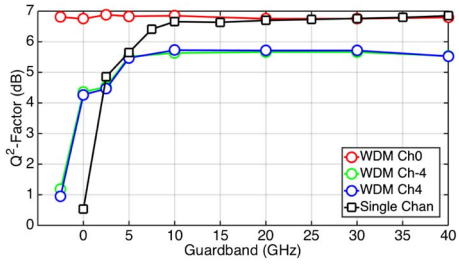

Fig. 4. Back-to-back performance for the central (Ch 0) and outermost subchannels (Ch ± 4) of the test superchannel with SS-ASE loading. Shown as squares is the performance of a single-channel system.

720 GHz of SS-ASE before transmission impairments. The effect of changing the SS-ASE's proximity to the superchannel (hence, guardband) was investigated, with the results shown in Fig. 4. The WSS used for shaping is not a perfect filter; see Fig. 3(b); it has a specified resolution of 12 GHz, a roll off of 1.0 dB/GHz, and a finite extinction ratio limit of 27 dB, which results in linear crosstalk, even for large guardbands. The Q-factor as a function of guardband between the superchannel and the SS-ASE for the central subchannel and outermost subchannels (±40 GHz relative to the central subchannel) is shown in Fig. 4. For guardbands greater than 10 GHz, the outermost subchannels (Ch ± 4) exhibited an additional penalty of 1 dB compared to the central subchannel (Ch 0). This penalty in performance is due to the limited effective number of bits in the analog-to-digital converters used in this work. When the guardband was less than 10 GHz, a penalty was observed on the outermost subchannels arising from linear crosstalk. The impact of the SS-ASE guardband when the superchannel was replaced with a single channel is also characterized. In this case, the impact can be seen occurring at just below 10 GHz, which is a larger guardband than that corresponding to the outermost subchannels. This is because a single channel is subject to crosstalk from both sides and the WSS resolution. When the guardband was larger than 10 GHz, the performance was unaffected by the SS-ASE as the only noise added arose from the WSS extinction ratio rather than its roll off. The spectral distance between the SS-ASE and the channel under test was minimized, to maximize spectral efficiency, but not incur a linear penalty; the transmission experiments were conducted with a guardband of 5 GHz.

To compare the impact of modulated interferers and SS-ASE-based interferers on the transmission performance in Fig. 5, the total transmission bandwidth was set to 90.1 GHz, equal to that of the nine subchannels of the superchannel. A transmission distance of 1225 km was chosen to give a BER of at least 5×10^{-3} for the central subchannel so that any change in performance could be readily measured.

For Fig. 5, the modulated outermost subchannels of the superchannel were progressively replaced with SS-ASE, while maintaining the total bandwidth of the "superchannel" at 90.1 GHz. The Q^2 factor of the central subchannel as a function of the launch power per subchannel is measured for the following configurations: one subchannel with 80 GHz of SS-ASE

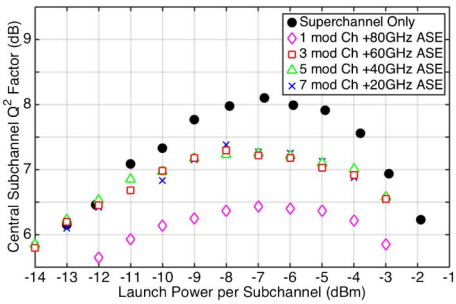

Fig. 5. Performance of the central channel in presence of SS-ASE interferer channels in PDM-16QAM transmission over 1225 km.

(diamonds), three subchannels and 60 GHz of SS-ASE (squares), five subchannels and 40 GHz of SS-ASE (triangles), seven subchannels and 20 GHz of SS-ASE (crosses), and a complete nine subchannel superchannel (filled circles). In the linear transmission regime (low launch powers), the performance of the superchannel only and the superchannel with up to six outer channels replaced with SS-ASE shows the same performance. We observe that when all but the central channel is replaced with SS-ASE, the performance in the linear regime is degraded; this is a result of the linear crosstalk arising from the 5 GHz guardband as shown in Fig. 4. In the nonlinear regime, where errors are dominated by nonlinear noise, a penalty in performance compared to the superchannel only result is incurred. This is manifested as a drop in peak Q^2 factor of 0.8 dB and a reduction in optimum launch power of 1 dB per subchannel. The SS-ASE gives rise to more noise in the nonlinear regime, as the peak-to-average ratio of the SS-ASE is larger than that of the PDM-16QAM signal at the beginning of the transmission link.

To assess over what distances this penalty is incurred, three and nine subchannels of modulated data were launched into the fiber and loaded with SS-ASE up to a total bandwidth 810 GHz [this is the maximum bandwidth that could be transmitted while maintaining −7 dBm/10 GHz the optimum launch power per channel], as shown in Fig. 6. This increased

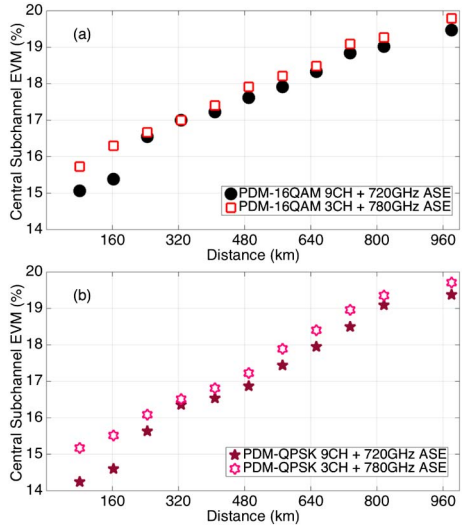

Fig. 6. Performance of (a) PDM-16QAM and (b) PDM-QPSK central subchannel in terms of EVM with eight or two like neighboring subchannels, maintaining total bandwidth with SS-ASE to 810 GHz.

bandwidth leads to greater nonlinearities and was used to highlight the difference in convergence distances of each scheme. The error vector magnitude (EVM) was measured for the central subchannel as a function of distance. EVM is used as the metric for performance at short distances as there are no errors to count. The modulated data channel formats in Fig. 6(a) and 6(b) are PDM-16QAM and PDM-QPSK, respectively. In the case of PDM-16QAM, it can be seen that at the start of transmission (up to 160 km, two spans), there is a discrepancy of 0.4% in EVM between the cases of data channels or ASE as interferers. The discrepancy also exists for PDM-QPSK, though the difference is larger at 1.1% and requires a longer propagation distance before the results converge. The convergence of the PDM-QPSK and PDM-16QAM EVM performance penalties to that of the SS-ASE at around 320 km for PDM-QPSK and 240 km for PDM-16QAM is consistent with the distances required for the PDM-QPSK and PDM-16QAM electric-field distributions to approach the Rayleigh distribution of the SS-ASE signal shown in Figs. 1 and 2.

In conclusion, the use of SS-ASE for investigation of system performance in spectrally efficient Nyquist-spaced WDM systems has been demonstrated to be an effective technique. When using SS-ASE as a substitute for interfering data channels over transmission distances longer than 320 km, we obtain a maximum Q^2 factor that is lower than that found when all subchannels are modulated with the same format. This underestimation of system performance (0.8 dB at 1200 km for PDM-16QAM) arises as a result of the disparity between the electrical-field distribution of modulated signals and the SS-ASE over the first few spans of the transmission. It is shown that the discrepancy decreases as the modulation order is increased and is expected to improve further for higher cardinalities (e.g., 64QAM and above). Thus, the use of SS-ASE to emulate the interfering channels provides a conservative estimate of system performance.

Funding. Engineering and Physical Sciences Research Council (EPSRC) (EP/J017582/1).

Acknowledgment. An EPSRC iCASE Ph.D. studentship award in collaboration with the BBC and support from the CNPQ-Brazil is gratefully acknowledged.

REFERENCES

1. R. Maher, T. Xu, L. Galdino, M. Sato, A. Alvarado, K. Shi, S. Savory, B. C. Thomsen, R. Killey, and P. Bayvel, Sci. Rep. **5**, 8214 (2015).
2. Y. Koizumi, K. Toyoda, M. Yoshida, and M. Nakazawa, Opt. Express **20**, 11 (2012).
3. T. Xu, J. Li, G. Jacobsen, S. Popov, A. Djupsjöbacka, R. Schatz, Y. Zhang, and P. Bayvel, Opt. Commun. **353** (2015).
4. J. X. Cai, H. Batshon, M. Mazurczyk, H. Zhang, Y. Sun, O. V. Sinkin, D. G. Foursa, and A. Pilipetskii, *Optical Fiber Communication Conference Post Deadline* (2015), paper Th5C.8.
5. H. Zhang, H. G. Batshon, C. R. Davidson, D. Foursa, and A. Pilipetskii, J. Lightwave Technol. **33**, 13 (2015).
6. M. E. McCarthy, N. Suibhne, S. Le, P. Harper, and A. D. Ellis, *European Conference on Optical Communication* (2014), paper P.5.7.
7. R. Dar, M. Feder, A. Mecozzi, and M. Shtaif, Opt. Express **21**, 25685 (2013).
8. A. Carena, G. Bosco, V. Curri, P. Poggiolini, M. Tapia Taiba, and F. Forghieri, *European Conference on Optical Communication* (2010), paper P4.07.